Shape from Heat Conduction - Supplementary Material

Sriram Narayanan[1], Mani Ramanagopal[1], Mark Sheinin[2], Aswin C. Sankaranarayanan[1], and Srinivasa G. Narasimhan[1]

[1] Carnegie Mellon University, USA
[2] Weizmann Institute of Science, Israel

A Deriving Transient Heat Equation

Consider an infinitesimal volume of our domain Ω as shown in the Fig. 1 where $\dot{E}_{st}$ be the rate of change of stored energy and $\dot{E}_g$ be the rate of generated energy inside this volume. We define conduction heat rates perpendicular to our infinitesimal volume in x, y and z directions by q_x, q_y, q_z, and heat rate at the corresponding opposite surface to be q_{x+dx}, q_{y+dy} and q_{z+dz}. According to the first law of thermodynamics, we can write the total energy conservation in the system as follows,

$$\dot{E}_{in} + \dot{E}_g - \dot{E}_{out} = \dot{E}_{st} \tag{1}$$

Substituting the respective quantities into the above equation we get,

$$q_x + q_y + q_z + \dot{q}\mathrm{dxdydz} - q_{x+dx} - q_{y+dy} - q_{z+dz} = \rho c_p \frac{\partial T}{\partial t}\mathrm{dxdydz} \tag{2}$$

where $\dot{q}$ is the rate of energy generated per unit volume in the medium (W/m^3), ρ is the density (kg/m^3) and c_p is the specific heat capacity of the solid $(J/(kg \cdot K))$. Now, we can then define first-order Taylor series expansion for heat rates at the opposite sides as,

$$\begin{aligned} q_{x+dx} &= q_x + \frac{\partial q_x}{\partial x}\mathrm{d}x \\ q_{y+dy} &= q_y + \frac{\partial q_y}{\partial y}\mathrm{d}y \\ q_{z+dz} &= q_z + \frac{\partial q_z}{\partial z}\mathrm{d}z \end{aligned} \tag{3}$$

The conduction rates within an isotropic medium can be evaluated through Fourier's law of heat conduction,

$$q = -kA\nabla T \tag{4}$$

where k is the thermal conductivity $(W/(m \cdot K))$, A is the surface area (m^2) and ∇T spatial temperature gradient (K/m). Substituting Eq. 3 into Eq. 4 and

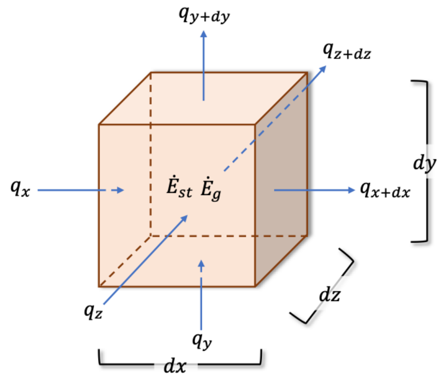

Fig. 1: An infinitesimal volume inside the object with sides dx, dy, dz where $\dot{E}_{st}$, $\dot{E}_g$ is rate of change of the energy stored and rate of change of the energy generated inside this volume respectively.

rearranging it, we get,

$$\begin{aligned} q_x - q_{x+dx} &= \mathrm{dxdydz}\Big(k\frac{\partial^2 T}{\partial x^2}\Big) \\ q_y - q_{y+dy} &= \mathrm{dxdydz}\Big(k\frac{\partial^2 T}{\partial y^2}\Big) \\ q_z - q_{z+dz} &= \mathrm{dxdydz}\Big(k\frac{\partial^2 T}{\partial z^2}\Big) \end{aligned} \tag{5}$$

here we have substituted for the cross-sectional area in the respective directions and the thermal conductivity k is assumed to be a constant. Plugging Eq. 5 back into the conservation of energy in Eq 2 and dividing out the infinitesimal volume we obtain,

$$\Big(\frac{\partial^2 T}{\partial x^2} + \frac{\partial^2 T}{\partial y^2} + \frac{\partial^2 T}{\partial z^2}\Big) + \frac{\dot{q}}{k} = \frac{1}{\alpha}\frac{\partial T}{\partial t} \tag{6}$$

where, $\alpha = k/\rho c_p$ is the thermal diffusivity (m^2/s). This is the transient heat conduction equation in a solid medium [3].

Boundary conditions. The above-mentioned Eq. 6 was derived for an infinitesimal volume inside the domain Ω regardless of the conditions on its surface $\partial\Omega$. While it models heat transfer through conduction within the domain, it does not account for heat transfer through other modes such as convection and radiation. In order to have a well-posed problem, we need to account for these heat transfer modes. Since both convection and radiation are surface phenomena, they are generally specified as boundary conditions.

Since a surface has no thickness and hence zero mass it cannot store energy. Therefore, any amount of heat entering the surface must exit on the other side.

This is mathematically expressed as,

$$-k\nabla T \cdot \hat{\mathbf{n}} = h_c(T - T_{surr}) + \sigma\epsilon(T^4 - T_{surr}^4) \quad (7)$$

where $\hat{\mathbf{n}}$ is the surface normal pointing out from the surface, h_c is the convective heat transfer coefficient $(W/(m^2 \cdot K))$, ϵ is the emissivity of the surface, σ is the Stefan-Boltzmann constant $(W/(m^2 \cdot K^4))$ and T_{surr} is the temperature of the surrounding medium. The left-hand side of the above equation represents the heat flux through the surface, from inside to outside, given by Fourier's law of heat conduction. The right-hand side represents the heat flux through the surface due to convection and radiation. The above equation simply states that heat conduction through a surface in a given direction is equal to the heat transfer through convection and radiation in the same direction.

Combined heat equation with boundary conditions. Energy conservation equation of an infinitesimal volume exposed to the surface with a surface area A and has no internal energy generation ($\dot{q} = 0$) can be written as,

$$\rho c_p \frac{\mathrm{dT}}{\mathrm{dt}}\mathrm{dv} \;=\; k\Delta T \;\mathrm{dv} + \sigma\epsilon A(T_{surr}^4 - T^4) + h_c A(T_{surr} - T) + \beta\phi_q \quad (8)$$

Here, we have merged the boundary condition and the energy conservation equation into one equation. Δ is the generalized Laplace-Beltrami operator that estimates Laplacian in a Partial Differential Equations (PDE). The last term represents energy input to the infinitesimal volume through external means where ϕ_q is the input power per unit area (W/m^2) and β is the energy absorption factor. Dividing out the infinitesimal volume and rearranging the terms we obtain,

$$\frac{\mathrm{dT}}{\mathrm{dt}} \;=\; \alpha\Delta T + \frac{1}{\rho c_p \mathrm{dv}}\Big(\sigma\epsilon A(T_{surr}^4 - T^4) + h_c A(T_{surr} - T) + A\beta\phi_q\Big) \quad (9)$$

If the infinitesimal volume is not exposed to any surface and the external energy input is only coming along the surface, then the above equation reduces to the transient heat conduction Eq. 6.

B Discussion and Limitations

Effect of material type on thermal observations: High thermal conductivity allows heat to reach faster to far away points on the object but reduces the amount of heat concentration. Hence, high-power light sources are needed for such materials to get a good SNR. High thermal conductivity also implies that the spatial gradient of temperature on an object is small impacting the Laplace operator estimation. In such cases, inducing heat using a source with high spatial frequency can introduce sufficient temperature differences observable by thermal cameras. Objects with low thermal conductivity can work with comparatively low-frequency sources but require longer durations to induce sufficient heat conduction.

Errors at Shape Boundaries: Our approach fails to accurately estimate Laplacian weights at the boundary since the heat travels beyond an object's silhouette. This causes the shape near the boundary to have comparatively large errors. But using simulations we validated that inaccurate Laplacian estimates near the boundary have minimal effect on heat flow at interior regions by comparing the forward model with a full bunny and one that is sliced at the silhouette boundary. Additionally, this issue can be mitigated by having multiple views for shape recovery and is a promising avenue of future work.

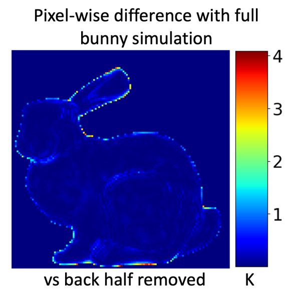

Effect of object's emissivity: Our work assumes the emissivity of objects is known, but it depends on a variety of factors such as material property, surface roughness, and viewing angle [3]. Moreover, polished surfaces are more reflective in thermal medium, and have low emissivity which makes temperature measurement hard for such objects. Note that materials like glass and acrylics that are transparent in the visible spectrum absorb infrared radiation and, hence, heat up. In theory, our approach does not depend on the visible BRDF, but in practice, SNR increases with the intensity of generated heat and the surface's emissivity.

C Operation of Thermal Cameras

Any object with a temperature above absolute zero emits thermal radiation. A thermal camera operates by converting the incoming radiation in the Long Wave Infrared (LWIR) spectrum into digital images. The total radiation emitted by a blackbody at temperature T_{bb} over all wavelengths is approximated using Stefan-Boltzmann law [1], which states that the total power emitted by a blackbody P_{bb} is proportional to the fourth power of its temperature.

$$P_{bb} = \sigma T_{bb}^4 \tag{10}$$

A thermal camera with a spectral response in LWIR region measures only a portion of this total radiation. Relating the power received by a thermal camera to the temperature of the object would require solving a complex double integral. This relation is typically approximated through a curve fitting with known temperature of the object and power received by the thermal cameras.

Sakumo-Hattori curve. Camera manufacturers generally use a variation Sakumo-Hattori equation to relate the temperature of the black body to the measured signal. This is given by,

$$T_{bb} = \frac{B}{\ln(\frac{R}{(U-J_0)/J_1} + F)} \tag{11}$$

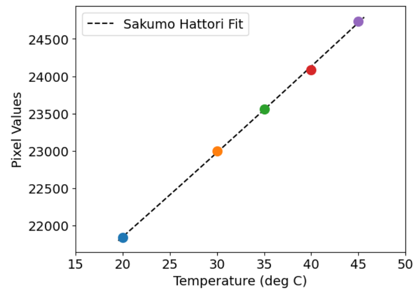

Fig. 2: Sakumo Hattori fit (Eq. 11) for a black body at different temperatures

where R, B, F, J_0 and J_1 are calibration parameters. Note that Eq. 11 returns the surface temperature that a blackbody must be at in order for the camera to produce the same pixel value U. In practice, the total thermal radiation reaching the camera includes several components like the emissivity ϵ of the object and also the surrounding temperature.

Incident radiant flux on thermal cameras. To thoroughly assess the elements of thermal radiation, one must account for emitted, reflected, and transmitted radiation at every interface between media along the optical ray originating from the camera. Nagase et al. [2] leveraged the transmission property of thermal radiation through multi-spectral measurements for shape recovery of objects. In cases where objects are within a few meters, the atmosphere can be deemed fully transmissive. Considering the emitted and reflected radiations, the total radiation captured by the thermal camera comprises of two components radiation emitted by the object, and the radiation reflected by it. The total radiant power that is received can then be written as,

$$W_{tot} = \epsilon_{obj} W_{obj} + (1 - \epsilon_{obj}) W_{surr} \tag{12}$$

here, ϵ_{obj} is the emissivity of the object and the radiation emitted due to the atmospheric temperature has been ignored since the atmosphere is considered to be fully transmissive. A similar expression can be written in terms of pixel counts as camera's measured signal is considered proportional to the input radiant power.

$$U_{tot} = \epsilon_{obj} W_{obj} + (1 - \epsilon_{obj}) U_{surr} \tag{13}$$

Thermal camera calibration. The radiometric calibration of thermal cameras is conducted by the camera manufacturer, utilizing blackbody sources arranged in a semi-circular configuration with varied, known temperature values. In this process, a thermal camera, mounted on a robotic arm, is directed towards each source, and the camera signal received for the known temperature measurements is recorded to establish a curve, as represented by Eq. 11. Over time, due to electronic aging, the calibration parameters may undergo a shift. To address this, we implement a straightforward calibration procedure using a blackbody set at known temperature values and re-fitting the camera response curve as illustrated in Fig. 2.

Estimating object's emissivity. The signal received by thermal cameras for an object at a specific temperature is significantly influenced by emissivity. Despite emissivity values for various materials being available online, it is still influenced by properties such as material roughness and viewing angle. A straightforward method to estimate the emissivity of a surface involves using a high-emissivity material, such as electrical tape, affixed to the object's surface. The ratio of counts received by the electrical tape section of the object compared to other regions provides a preliminary estimate of the object's emissivity.

References

1. Bergman, T.L.: Introduction to Heat Transfer. Wiley (2011)
2. Nagase, Y., Kushida, T., Tanaka, K., Funatomi, T., Mukaigawa, Y.: Shape from thermal radiation: Passive ranging using multi-spectral lwir measurements. In: 2022 IEEE/CVF Conference on Computer Vision and Pattern Recognition (CVPR). pp. 12651–12661 (2022). https://doi.org/10.1109/CVPR52688.2022.01233
3. Vollmer, M., Mllmann, K.P.: Some Basic Concepts in Heat Transfer, chap. 4, pp. 351–392. John Wiley & Sons, Ltd (2017). https://doi.org/10.1002/9783527693306.ch4